

RESEARCH ARTICLE



Cucurbitacin B regulates lung cancer cell proliferation and apoptosis *via* inhibiting the IL-6/STAT3 pathway through the lncRNA XIST/miR-let-7c axis

Jian-Hua Liu, Chen Li, Liang Cao, Chang-Hong Zhang and Zhi-Hua Zhang

Department of Respiratory Medicine, The First Affiliated Hospital of Hebei North University, Zhangjiakou, Hebei, China

ABSTRACT

Context: Lung cancer, the most common type of cancer, has a high mortality rate. Cucurbitacin B (CuB), a natural compound extracted from Cucurbitaceae plants, has antitumor effects.

Objective: We investigated the role of CuB on lung cancer and its potential mechanisms.

Materials and methods: A549 cells were treated with 0.1, 0.3, 0.6, and 0.9 μ M CuB for 12, 24, and 48 h or untreated. Gene and protein levels were evaluated by quantitative real-time polymerase chain reaction (qRT-PCR) and western blotting. Enzyme-linked immunosorbent assay (ELISA) detected inflammatory factors levels (TNF- α and IL-10). 3-(4,5-Dimethylthiazol-2-yl)-2,5-diphenyltetrazolium bromide (MTT), flow cytometry, and colony formation assays measured cell viability, apoptosis, and proliferation. The interaction between miR-let-7c and long non-coding RNA X inactive-specific transcript (XIST) or interleukin-6 (IL-6) was verified by dual-luciferase reporter assays.

Results: CuB treatment inhibited the proliferation of lung cancer cells and promoted cell apoptosis, and increased the expression of Bax and cleaved caspase3, decreased cyclin B1 and Bcl-2 expression. CuB suppressed XIST and IL-6 expression, and enhanced miR-let-7c expression. XIST silencing enhanced the inhibitory effect of CuB on cell proliferation and the promotion effect on apoptosis *via* upregulating miR-let-7c. Moreover, XIST targeted miR-let-7c to activate the IL-6/STAT axis. MiR-let-7c overexpression enhanced the regulatory effect of CuB on proliferation and apoptosis *via* suppressing the IL-6/STAT3 pathway.

Discussion and conclusion: CuB regulated cell proliferation and apoptosis by inhibiting the XIST/miR-let-7c/IL-6/STAT3 axis in lung cancer. These findings indicate CuB may have the possibility of clinical application in lung cancer treatment.

ARTICLE HISTORY

Received 22 February 2021
Revised 26 October 2021
Accepted 4 December 2021

KEYWORDS

CeRNA; lncRNA-miRNA-mRNA axis; antitumor drug

Introduction

Lung cancer is the most common tumour worldwide, with a high mortality rate (Bray et al. 2018). Data show that lung cancer deaths account for 20% of cancer deaths, and its mortality rate ranks first among all types of tumours (Bray et al. 2018). Studies have demonstrated that the occurrence and development of cancer are closely related to genes, and many genes are abnormally expressed in tumours, which are also commonly referred to as oncogenes (Schaefer and Serrano 2016). Therefore, it is of great significance to explore the molecular mechanism of lung cancer and formulate related treatment strategies.

Natural compounds of plant origin and their related derivatives are of great significance for the development of cancer treatment drugs (Zhou et al. 2017). Cucurbitacin, a natural compound, plays a key role in the treatment of diseases (Chan et al. 2010). Cucurbitacin is divided into cucurbitacin A-T, and cucurbitacin B (CuB) is the most common type (Chen et al. 2005). As widely reported, CuB has good antitumor activity (El-Senduny et al. 2016). Chen et al. (2005) revealed CuB had low toxicity to normal cells and could induce gastric cancer cell apoptosis. Additionally, CuB treatment was reported to inhibit tumour proliferation and invasion by inducing G2/M phase arrest (Guo et al. 2014). However, the specific antitumor mechanism of CuB

is not clear. Herein, we explore the specific mechanism of CuB in lung cancer.

Non-coding RNAs (ncRNAs) refer to those RNAs without the coding ability (Dong et al. 2018), and ncRNAs with a length of more than 200 nt are called long non-coding RNA (lncRNA) (Iyer et al. 2015). LncRNAs play critical roles in various biological processes. More importantly, it is shown in the literature that lncRNAs were closely related to the occurrence and development of lung cancer (Luo et al. 2015). LncRNA X-inactive specific transcript (XIST) is the first discovered long non-coding RNA associated with cancer, which is abnormally expressed in many tumours (Sun et al. 2018; Zheng R et al. 2018). As previously reported, XIST was upregulated in lung cancer (Zhu et al. 2018). Fang et al. (2016) also revealed that XIST knockdown impaired non-small cell lung cancer (NSCLC) cell proliferation, migration, and invasion *in vitro*, and repressed the tumorigenicity of NSCLC cells *in vivo*. In addition, XIST silencing was probed to inhibit NSCLC cell growth and enhance the chemosensitivity to cisplatin (Xu X et al. 2020). However, the molecular mechanism of XIST affecting lung cancer is still under-reported and needs further exploration.

MicroRNAs (miRNAs) are endogenous short RNAs (21–25 nt), which regulate gene expression post-transcriptionally. It's well-known that lncRNAs can participate in the development

of cancer by sponging miRNAs (Wang et al. 2017). It was reported that miR-let-7c was downregulated in lung cancer (Wu et al. 2016). We predicted that XIST had a binding site to miR-let-7c by using bioinformatics analysis. However, its specific mechanism in lung cancer needs to be further explored. Inflammatory factors (interleukin-6, IL-10, and TNF- α) are reported to be of importance in the development of lung cancer (Seifart et al. 2005). Epithelial-mesenchymal transition (EMT) in NSCLC was associated with increased expression of multiple immunosuppressive cytokines, including IL-10 (Chae et al. 2018). Interleukin-6 and TNF- α were also reported to promote metastasis of lung cancer by inducing EMT (Shang et al. 2017). IL-6/signal transducer and activator of transcription (STAT) 3 signalling pathway regulates a series of biological processes, such as cell proliferation, apoptosis, and invasion *in vivo* (Yu et al. 2018). In recent years, the IL-6/STAT3 pathway has become a hot spot in cancer research. Studies showed that the IL-6/STAT3 pathway was abnormally upregulated in lung cancer, thereby mediating lung cancer cell proliferation and invasion (Yu et al. 2018). MiRNA works by binding to the 3'-untranslated region (UTR) of the target mRNA, resulting in mRNA degradation and inhibiting protein translation (Bhatt et al. 2011). Herein, we found that miR-let-7c had a binding site to IL-6. Thus, we speculated that XIST played the role in the development of lung cancer by regulating the IL-6/STAT3 signal axis *via* targeting miR-let-7c.

Our results suggested that CuB could obviously suppress the proliferation of lung cancer cells and induce apoptosis. Moreover, XIST silencing significantly enhanced the effect of CuB on lung cancer by regulating the IL-6/STAT3 pathway *via* targeting miR-let-7c, which provided a potential target for the treatment of lung cancer in the future.

Materials and methods

Cell culture

A549 cell was obtained from American Type Culture Collection (ATCC, VA, USA). Cells were cultured in Dulbecco's modified Eagle media (DMEM, Gibco, CA, USA) with 10% fetal bovine serum (FBS, Gibco). Cells were cultured at 37°C, in a humidified atmosphere with 5% CO₂.

Plasmid construction and transfection

Plasmid DNA-encoding IL-6 was constructed by inserting the cDNA clone of IL-6 into the pcDNA3.1 vector (Life Technologies, CA, USA). The short hairpin RNA against XIST (sh-XIST) and its negative control (shNC) were purchased from GenePharma (Shanghai, China). And miR-let-7c mimics/inhibitor and mimics/inhibitor NC were obtained from Sigma-Aldrich (CA, USA). For *in vitro* transfection, cells were transfected using Lipofectamine™ 3000 (Sigma-Aldrich, MO, USA) according to the manufacturer's instructions.

3-(4,5-Dimethylthiazolyl)-2,5-diphenyltetrazolium bromide (MTT) assay

Cells were suspended in complete DMEM medium mixed with 5 mg/mL MTT and then incubated at 37°C for 4 h. After incubation, the medium was removed. Then dimethyl sulfoxide (DMSO) was added and the absorbance at 490 nm was detected by a microplate reader (Bioteke, Beijing, China). The absorbance value relative to the control was taken as the relative cell viability.

Flow cytometry assay

Cell apoptosis was determined by Annexin V-FITC/PI Apoptosis Detection Kit (Yeasen, Shanghai, China) in accordance with the instruction. After treatment, cells were digested and harvested. Then cells were washed twice with pre-chilled PBS. PBS was removed and cells were resuspended in 100 μ L of 1 \times binding buffer. Cells were then incubated with 5 μ L Annexin V-FITC and 10 μ L PI staining solution protected from light at room temperature. After the 10 min incubation, samples were analyzed using FlowJo V7 software V7 software (TreeStar, OR, USA).

Enzyme-linked immunosorbent assay (ELISA)

The levels of TNF- α and IL-10 were determined by ELISA kits (Abcam, Cambridge, UK). Specifically, the cell supernatant was collected. 20 μ L of cell supernatant, 30 μ L of sample dilution, and 100 μ L of HRP were added to each well of the antibody-coated plate and incubated the plate for 1 h at 37°C in the dark. Then the liquid was removed from the microplate. Each well of the microplate was filled with the washing solution, and pated the microplate dry after draining the washing solution. The above operation was repeated five times. 50 μ L of the reaction solution was added to each well and incubated the plate for 30 min at 37°C prevented from light. Then 50 μ L of stop solution was added to each well, and the absorbance of each well was measured at 450 nm.

Colony formation assay

For colony formation analysis, 1 \times 10³ A549 cells were seeded in a 6-well plate (Corning, NY, USA) and incubated for 2 weeks at 37°C. Then, cells were washed twice in PBS, fixed with 4% formaldehyde for 15 min and stained with 0.1% crystal violet, and the colonies formed were counted manually.

Luciferase reporter assay

We predicted the binding site between XIST, miR-let-7c, and IL-6 using common online tools, starBase (<http://starbase.sysu.edu.cn/>) and RAID v2.0 (<http://www.rna-society.org/raid/search.html>). The fragment of human XIST was amplified by PCR. Site-directed mutagenesis of the miR-let-7c binding site in the fragment of XIST was performed using a site-directed mutagenesis kit (Stratagene, CA, USA). Wild-type (wt) and mutant-type (mut) reporter plasmids of XIST sequences were cloned into the pmirGLO Dual-Luciferase vector (Promega, WI, USA). Similarly, the wt/mut sequences from IL-6 3'-UTR containing the predicted miR-let-7c binding site were inserted into the pmirGLO Dual-Luciferase vector to construct IL-6-WT/IL-6-MUT. Then the XIST-WT/IL-6-WT vector or the XIST-MUT/IL-6-MUT vector and miR-let-7c mimics or mimics NC were co-transfected into cells. After 48 h of transfection, luciferase activity was detected by using a Dual-Luciferase Reporter Assay System (Promega).

Quantitative real-time polymerase chain reaction (qRT-PCR)

Total RNA was extracted from cells using TRIzol reagent (Invitrogen, CA, USA). Subsequently, the optical density values of A260 and A280 nm wavelengths were measured by an ultra-micro ultraviolet-visible spectrophotometer. The RNA concentration was calculated by the absorbance at 260 nm and the ratio of 260/280 nm was used to characterize the purity of RNA. cDNA was

synthesized using a HiFiScript cDNA synthesis kit according to the manufacturer's instruction (Life Technologies, CA, USA). The cDNA was used for qRT-PCR with specific primers for different genes. qRT-PCR reactions were conducted on an Eppendorf MasterCycler RealPlex4 (Eppendorf, Wesseling-Berzdorf, Germany) using an Ultra SYBR Mixture kit (Thermo Fisher Scientific, MA, USA). The relative expression of miRNA and mRNA were respectively normalized by U6 and GAPDH and calculated by $2^{-\Delta\Delta CT}$ method. The primers used for qRT-PCR were listed as follows:

- XIST F: 5'-CCTGTACGACCTAAATGTCC-3'
- XIST R: 5'-GTATTAGTGTGCGGTGTTGC-3'
- miR-let-7c F: 5'-GAGGTAGTAGTTGTATG-3'
- miR-let-7c R: 5'-GAACATGTCTGCGTATCTC-3'
- IL-6 F: 5'-TTCTACAGACTACGGTTTGAG-3'
- IL-6 R: 5'-GGATGACACAGTGATGCT-3'
- GAPDH F: 5'-GCACAGTCAAGGCCGAGAAT-3'
- GAPDH R: 5'-GCCTTCTCCATGGTGGTAA-3'
- U6 F: 5'-CTCGCTTCGGCAGCAC-3'
- U6 R: 5'-AACGCTTCACGAATTTGCGT-3'

Protein extraction and Western blotting

The protein was extracted from cells by RIPA mixed with 1% protease inhibitor and phosphorylase inhibitor, and the concentrations of protein were examined by a BCA Kit (Beyotime, Shanghai, China). Samples were separated using SDS-PAGE and then transferred onto a PVDF membrane. The blots were blocked with antibody blocking solution and then incubated overnight with primary antibodies against cyclin B1 (1:1000, ab181593, Abcam), Bax (1:1000, ab32503, Abcam), Bcl-2 (1:1000, ab182858, Abcam), and cleaved caspase-3 (1:1000, ab2302, Abcam). Anti-GAPDH antibody (Sigma-Aldrich) was used as a loading control. After being washed with PBS-T, membranes were then incubated with the corresponding secondary antibody labelled with HRP for 60 min. The membranes were covered with ECL Reagents (Beyotime) and the images were performed by a GEL imaging system (Bio-Rad, CA, USA). The quantification of proteins was analyzed by the software Image J.

Data analysis

All data are expressed as mean \pm standard deviation (SD) of at least three independent repetitions. Data were analyzed using one-way analysis of variance (ANOVA) and Student's *t*-test. Analysis was conducted using IBM SPSS Statistics 23 (IBM, NY, USA). The $p < 0.05$ was considered statistically significant.

Results

CuB inhibited cell proliferation and promoted apoptosis of lung cancer cells

Firstly, we treated A549 with 0.1, 0.3, 0.6, and 0.9 μ M CuB for 12, 24, and 48 h. The results of the MTT assay displayed that the viability of lung cancer cells gradually decreased with the increase of CuB concentration (Figure 1(A)). To further explore the effect of CuB, A549 cells treated with 0.1, 0.2, and 0.3 μ M CuB or without CuB, then clone formation assay was performed. As shown in Figure 1(B), cell proliferation of lung cancer cells was gradually reduced by the increase of CuB concentration. Moreover, results of the flow cytometry assay indicated that apoptotic lung cancer cells gradually enhanced with the increase

of CuB concentration (Figure 1(C)). And the protein levels of cyclin B1 and Bcl-2 in lung cancer cells gradually decreased with the increase of CuB concentration, while Bax and cleaved caspase 3 levels gradually increased (Figures 1(D,E)). In the next experiments, we selected 0.3 μ M CuB to treat A549 cells. Results showed CuB inhibited cell proliferation and promoted apoptosis of lung cancer cells.

CuB inhibited the expression of XIST and IL-6 in lung cancer cells and promoted the expression of miR-let-7c

The expression of XIST and IL-6 in A549 cells was markedly reduced by CuB treatment, while miR-let-7c expression was significantly upregulated (Figures 2(A-C)). Western blotting results showed that the level of STAT3 phosphorylation significantly decreased in CuB-treated A549 cells (Figures 2(D,E)). Results suggested that CuB could inhibit XIST expression and IL-6/STAT3 signalling pathway in lung cancer cells and promote miR-let-7c expression.

Knockdown of XIST could enhance the effect of CuB on proliferation and apoptosis of lung cancer cells

The expression of XIST was significantly reduced by sh-XIST transfection (Figure 3(A)). As displayed in Figure 3(B), XIST silencing could further inhibit cell viability of CuB-treated A549 cells, while miR-let-7c inhibition presented the opposite effect; and miR-let-7c knockdown reversed the inhibitory effect of sh-XIST on CuB-treated A549 cell viability (Figure 3(B)). In addition, XIST knockdown further reduced TNF- α and enhanced IL-10 levels in CuB-treated A549 cells, and miR-let-7c inhibitor transfection showed the opposite effects; inhibition of miR-let-7c abolished the inhibitory effects of sh-XIST on inflammatory factors levels in CuB-treated A549 cells (Figure 3(C)). Results from colony formation and flow cytometry assays subsequently demonstrated that downregulation of XIST enhanced the inhibition of CuB on cell proliferation and the promotion of CuB on cell apoptosis of A549 cells, while inhibition of miR-let-7c presented the opposite effects; and miR-let-7c inhibitor attenuated the effects of sh-XIST on cell proliferation and apoptosis of CuB-treated A549 cells (Figures 3(D,E)). Furthermore, knockdown of XIST further elevated Bax and cleaved caspase 3 levels and reduced cyclin B1 and Bcl-2 in CuB-treated A549 cells, whereas miR-let-7c knockdown presented the opposite effects; and miR-let-7c inhibition abolished the regulatory effects of sh-XIST on these proteins' expressions in CuB-treated A549 cells (Figures 3(F,G)). In total, the above results showed that knockdown of XIST promoted the effect of CuB on proliferation and apoptosis of lung cancer cells by targeting miR-let-7c.

XIST targeted miR-let-7c to positively regulate IL-6/STAT3 pathway

We screened miRNAs containing binding sites with XIST and IL-6 by bioinformatics software (starBase and RAID v2.0) (Figure 4(A)). Through the pre-experiment, we found that the expression of miR-let-7c in A549 cells was significantly elevated by CuB treatment, while there was no obvious change in the other targeted miRNAs (Figure 4(B)). To explore the relationship between miR-let-7c and XIST or IL-6, we predicted the binding site of XIST to miR-let-7c, and the binding site of miR-let-7c to IL-6 (Figure 4(C)). The dual-luciferase reporter gene assay

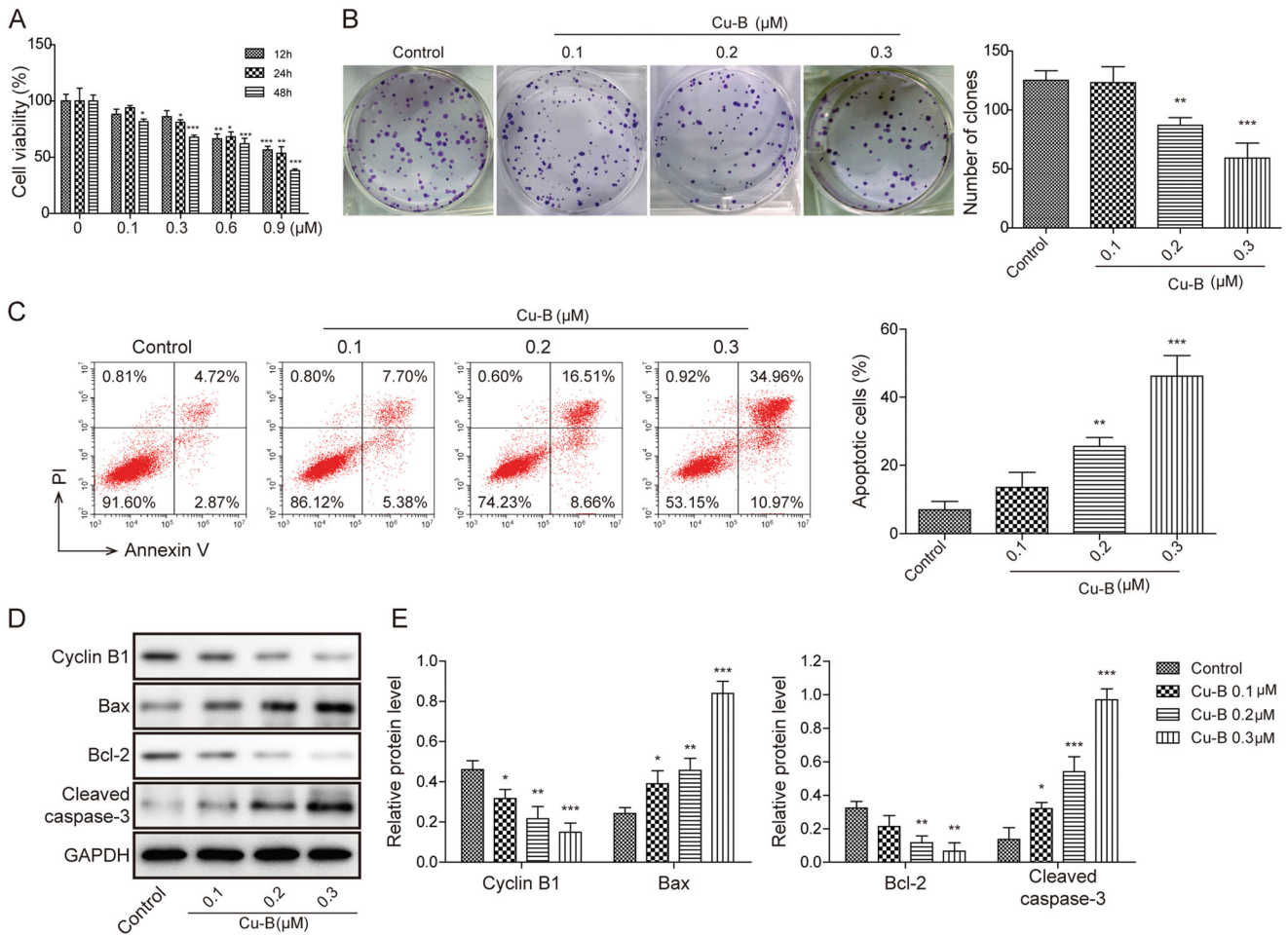


Figure 1. CuB inhibited cell proliferation and promoted apoptosis of lung cancer cells. (A) The viability of A549 treated with 0.1, 0.3, 0.6, and 0.9 μM CuB for 12, 24, and 48 h were detected by MTT. A549 cells were treated with 0.1, 0.2, 0.3 μM CuB for 48 h. (B) Colony formation assay detected cell proliferation of A549. (C) Flow cytometry determined cell apoptosis. (D,E) The protein levels of cyclin B1, Bax, Bcl-2, and cleaved caspase 3 were detected using western blotting. Results are expressed as mean ± SD. * $p < 0.05$, ** $p < 0.01$, *** $p < 0.001$.

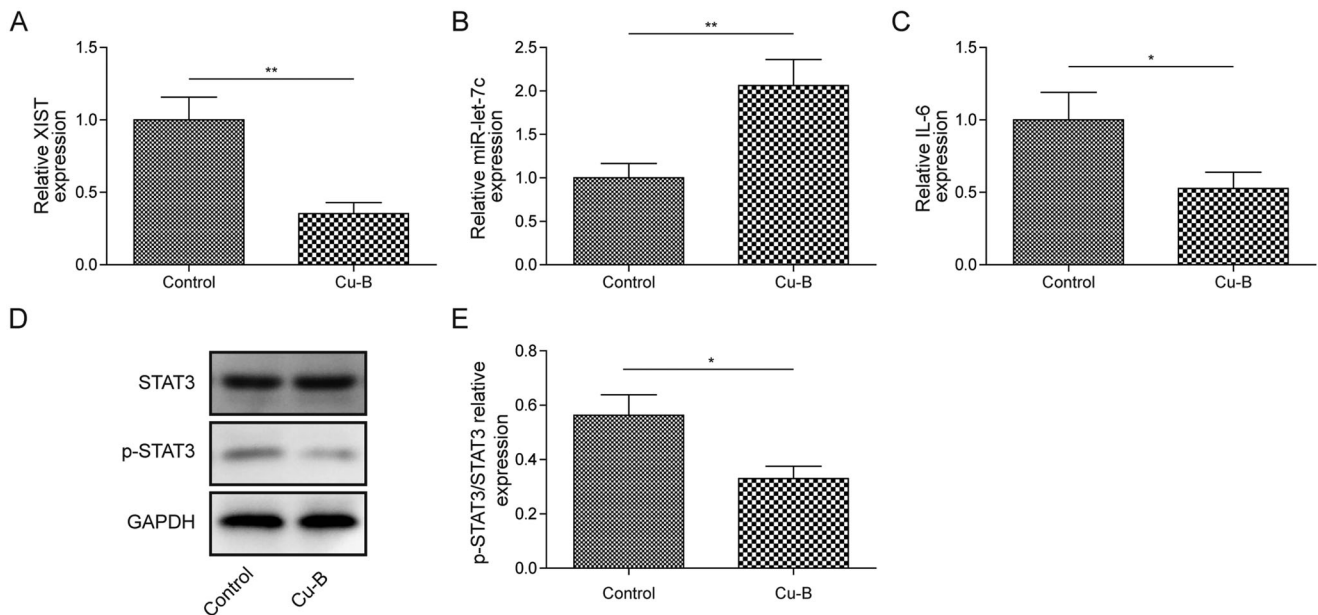


Figure 2. CuB inhibited the expression of XIST and IL-6 in lung cancer cells and promoted the expression of miR-let-7c. A-C, the expression levels of XIST (A), miR-let-7c (B), and IL-6 (C) in A549 after treatment of 0.3 μM CuB for 48 h was assessed using qRT-PCR. (D,E) The protein levels of STAT3 and p-STAT3 in A549 after treatment of 0.3 μM CuB for 48 h were detected using western blotting. Results are expressed as mean ± SD. * $p < 0.05$, ** $p < 0.01$.

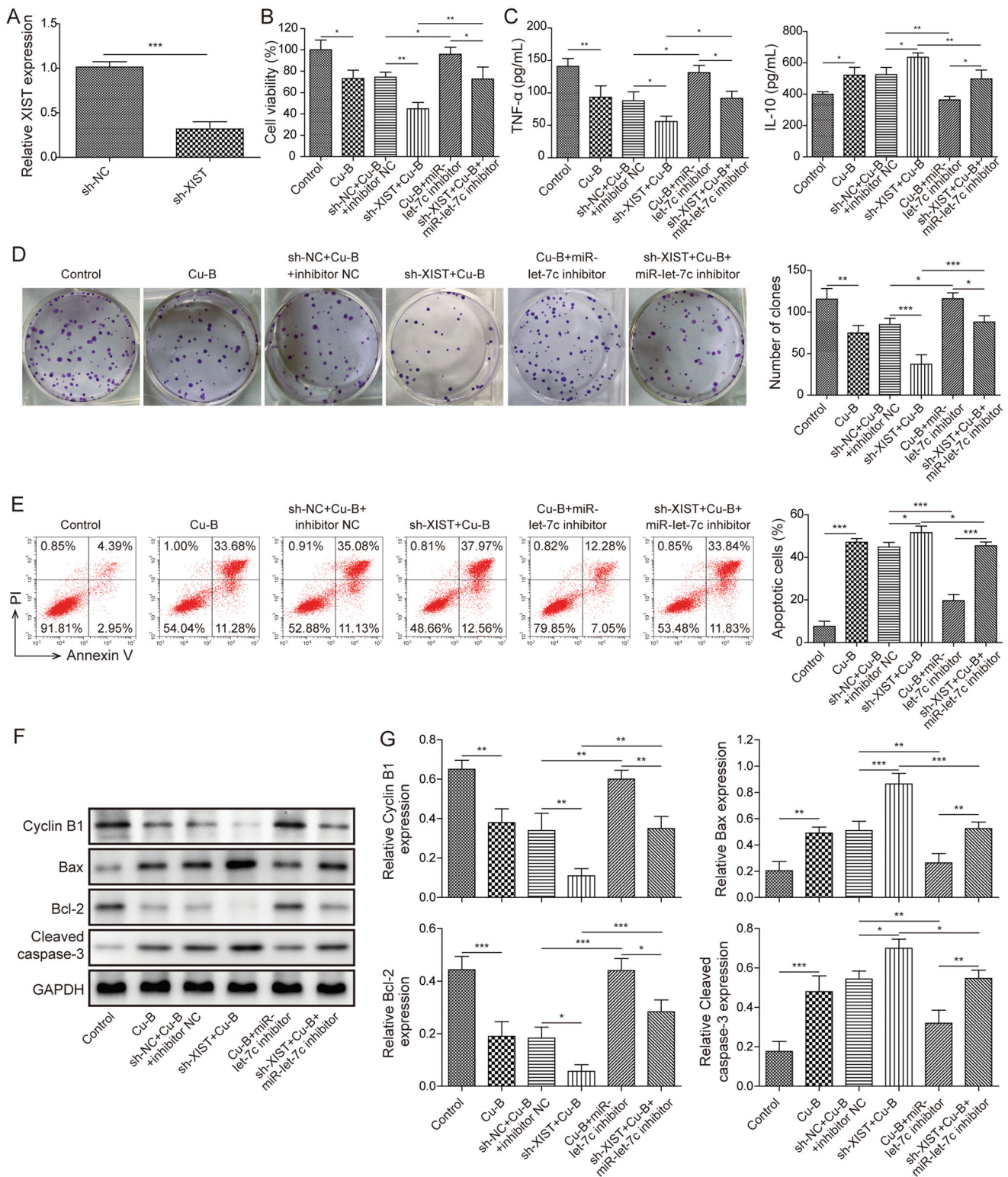


Figure 3. Knockdown of XIST could promote the effect of CuB on proliferation and apoptosis of lung cancer cells. A549 cells were transfected with sh-XIST or miR-let-7c inhibitor or co-transfected with sh-XIST and miR-let-7c inhibitor after treatment of 0.3 μ M CuB for 48 h. (A) The expression level of XIST in A549 was detected by qRT-PCR. (B) The viability of A549 was detected by MTT. (C) The levels of IL-10 and TNF- α in A549 were detected by ELISA. (D) Cell proliferation of A549 was detected by colony formation assay. (E) Cell apoptosis in A549 was detected by Flow cytometry. (F,G) The protein levels of cyclin B1, Bax, Bcl-2, and cleaved caspase-3 in A549 were detected by western blotting. Results are expressed as mean \pm SD. * p < 0.05, ** p < 0.01, *** p < 0.001.

showed that wild-type XIST and miR-let-7c mimics combined to reduce the luciferase activity, while the luciferase activity of mutant XIST was not significantly different, and wild-type IL-6 and miR-let-7c mimics combined to reduce the luciferase

activity, while the luciferase activity of mutant IL-6 was not changed (Figure 4(D)). The expression of miR-let-7c in A549 cells significantly increased after the knockdown of XIST (Figure 4(E)). Moreover, the level of miR-let-7c was markedly

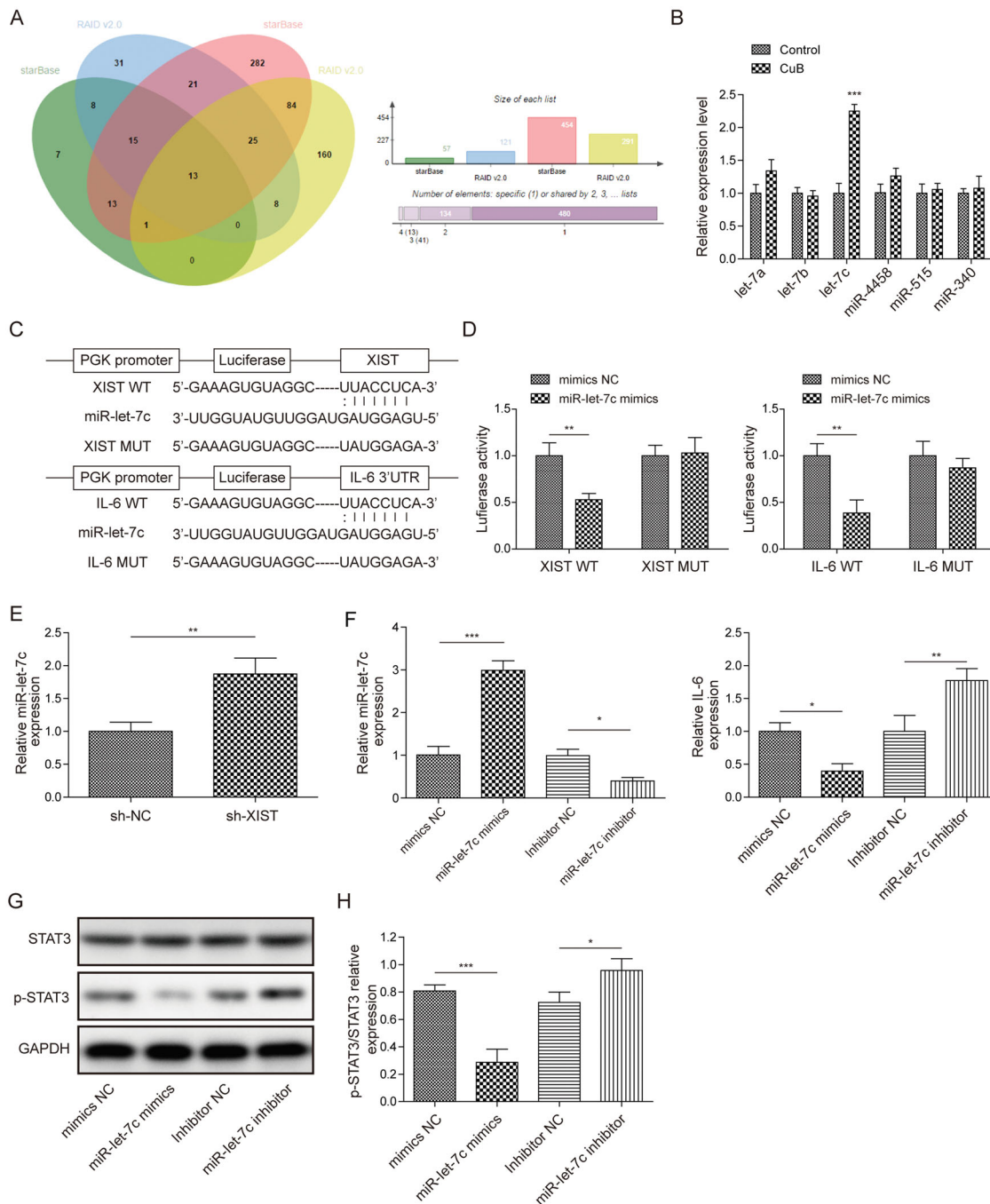


Figure 4. XIST targeted miR-let-7c to positively regulate the IL-6/STAT3 pathway. (A) Bioinformatics software predicted the miRNAs interacting with both XIST and IL-6. (B) qRT-PCR analysis of six miRNA expressions in CuB treated A549 cells. (C) Bioinformatics analysis the binding site between XIST and miR-let-7c, IL-6 was the target gene of miR-let-7c. (D) The interaction of XIST to miR-let-7c and IL-6 to miR-let-7c was assessed by dual-luciferase reporter gene assay. (E,F) A549 cells were transfected with sh-NC or sh-XIST or miR-let-7c inhibitor or miR-let-7c mimics or inhibitor NC or mimics NC for 24 h, then the levels of miR-let-7c and IL-6 in A549 was detected by qRT-PCR. (G,H) the protein levels of STAT3 and p-STAT3 in A549 after miR-let-7c knockdown or miR-let-7c overexpression was determined by western blotting. Results are expressed as mean \pm SD. * $p < 0.05$, ** $p < 0.01$, *** $p < 0.001$.

upregulated after miR-let-7c overexpression and was downregulated after the knockdown of miR-let-7c (Figure 4(F)). Moreover, the mRNA level of IL-6 was markedly reduced following miR-let-7c overexpression, while was obviously elevated by miR-let-7c inhibition (Figure 4(F)). Western blotting showed miR-let-7c overexpression suppressed the protein level of p-STAT3, while knockdown of miR-let-7c showed the opposite effect (Figures 4(G,H)). Taken together, XIST targeted miR-let-7c to positively regulate the IL-6/STAT3 pathway.

Overexpression of miR-let-7c promoted the regulation of CuB on lung cancer cells through IL-6/STAT3 axis

The expression of miR-let-7c and IL-6 was measured using qRT-PCR. Our results displayed that overexpression of miR-let-7c resulted in increased miR-let-7c expression and reduced IL-6 expression in CuB-treated A549 cells (Figure 5(A)). CuB could inhibit cell viability, and the inhibition rate of cell viability was higher after miR-let-7c overexpression, however, overexpression of IL-6 reversed the effect of miR-let-7c mimics (Figure 5(B)).

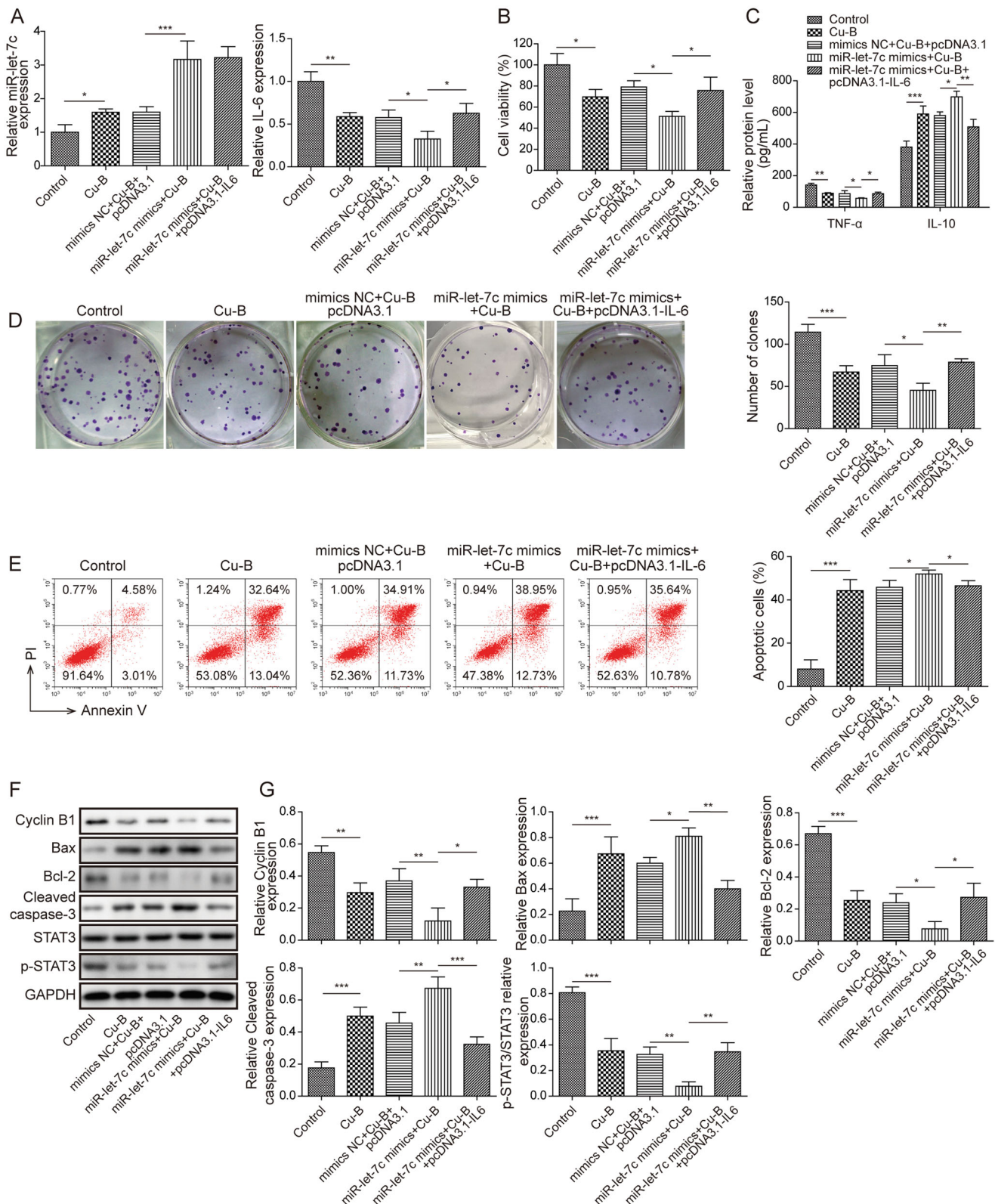


Figure 5. Overexpression of miR-let-7c improved the regulation of CuB on lung cancer cells through the IL-6/STAT3 axis. A549 cells were transfected with miR-let-7c mimics or co-transfected with miR-let-7c mimics and pcDNA3.1-IL-6 after treatment of 0.3 μ M CuB for 48 h. (A) The expression levels of miR-let-7c and IL-6 were assessed using qRT-PCR. (B) The viability of A549 was detected by MTT. (C) The levels of IL-10 and TNF- α was detected by ELISA. (D) Cell proliferation was detected by colony formation assay. (E) Cell apoptosis was detected by Flow cytometry. (F,G) The protein levels of cyclin B1, Bax, Bcl-2, cleaved caspase 3, STAT3, and p-STAT3 were detected using western blotting. Results are expressed as mean \pm SD. * p < 0.05, ** p < 0.01, *** p < 0.001.

CuB decreased the level of TNF- α and enhanced IL-10 level, overexpression of miR-let-7c further enhanced the regulatory effect of CuB on inflammatory factor expression, however,

overexpression of IL-6 reversed the effect of miR-let-7c mimics (Figure 5(C)). Cell proliferation was detected by colony formation assay and the data demonstrated that overexpression of

miR-let-7c enhanced the inhibitory effect of CuB on cell proliferation (Figure 5(D)). CuB promoted cell apoptosis, overexpression of miR-let-7c further induced the apoptosis, while overexpression of IL-6 reversed miR-let-7c mimics's promoting effect (Figure 5(E)). Furthermore, CuB increased the protein levels of Bax and cleaved caspase 3, decreased the protein levels of cyclin B1, Bcl-2, and p-STAT3, and overexpression of miR-let-7c further enhanced this regulatory effect of CuB, while overexpression of IL-6 alleviated the effect of miR-let-7c mimics in CuB treated A549 cells (Figures 5(F,G)). In short, results showed overexpression of miR-let-7c enhanced the regulation of CuB on lung cancer cells by the IL-6/STAT3 pathway.

Discussion

Lung cancer is the most common type of tumour, and the number of lung cancer patients is increasing by 1.04 million per year worldwide (Alberg and Samet 2003). The five-year survival rate of lung cancer patients is currently only 16%. In addition, the existing therapies for lung cancer have major drawbacks, mainly non-specificity and toxicity (Sharma et al. 2019). CuB is a natural compound that has been reported to have a tumour suppressive effect (Lai et al. 1989; Xu J et al. 2020). However, the molecular mechanism of CuB regulating the development of lung cancer is unclear. Herein, our results displayed that CuB could inhibit cell proliferation and induce apoptosis *via* inhibiting the XIST/miR-let-7c/IL-6/STAT3 axis in lung cancer.

It's well-known that CuB has a strong inhibitory effect on tumour development *in vivo* and *in vitro*, such as breast cancer, lung cancer, etc. (Garg et al. 2018). For instance, Dandawate et al. (2020) demonstrated that cucurbitacin B repressed the growth of colon cancer by inhibiting the Notch signalling pathway. A previous study displayed that CuB could suppress cell migration and invasion and induce cell apoptosis in lung cancer (Liu et al. 2019). Consistent with our result, we found that CuB inhibited cell proliferation and promoted cell apoptosis. Moreover, CuB promoted the expression levels of Bax and cleaved caspase 3, and inhibited Bcl-2 and cyclin B1 expression.

Increasing evidence suggests that abnormal expression of lncRNAs play key roles in the progression of various cancers (Prensner and Chinnaiyan 2011). Zheng P et al. (2018) displayed that lncRNA HOTAIR promoted migration and invasion of Hela cells. In addition, Lin et al. (2018) demonstrated that CuB could regulate the development of cancer *via* regulation of expression of lncRNA, specifically CuB promoted cell apoptosis of gastric cancer cells *via* downregulating lncRNA GACAT3. The XIST we studied here has been reported to have carcinogenic effects in a variety of cancers (Zhu et al. 2018). More importantly, XIST was reported to be upregulated in NSCLS, and XIST silencing obviously suppressed cell proliferation and invasion, and promoted apoptosis of lung cancer cells (Zhang et al. 2017). It was also reported that XIST promoted growth and metastasis of lung cancer *via* interacting with miR-140 (Tang et al. 2017). In this study, we demonstrated that CuB could downregulate the expression of XIST, and knockdown of XIST could enhance the regulatory effect of CuB on the proliferation and apoptosis in lung cancer cells. All our results suggested that CuB inhibited cell proliferation and induced apoptosis of lung cancer cells *via* reducing XIST expression, then we explored the downstream molecules of XIST.

Numerous studies have revealed that lncRNAs work by binding to miRNAs (Zhu et al. 2018). MiRNAs also act as an important role in tumorigenesis. For example, lncRNA H19

could induce cell proliferation and invasion of glioma cells *via* downregulating miR-675 (Shi et al. 2014). MiR-let-7c was reported to be downregulated in many human malignant tumours, and miR-let-7c overexpression could inhibit the growth of cancer by targeting various oncogenes (Tang et al. 2019). Additionally, low expression of miR-let-7c was observed in lung adenocarcinoma and was related to poor survival (Wang et al. 2020). However, the specific roles of miR-let-7c in regulating the process of lung cancer remains unclear. Herein, we found that XIST had a binding site to miR-let-7c, and overexpression of XIST could downregulate the expression of miR-let-7c. What's more, CuB could upregulate the expression of miR-let-7c, and overexpression of miR-let-7c could inhibit cell proliferation and promote cell apoptosis, suggesting that miR-let-7c mimics enhanced the inhibitory effect of CuB on cell proliferation and the promotion of apoptosis in lung cancer cells. Therefore, we concluded that CuB regulated lung cancer cell proliferation and apoptosis through the XIST/miR-let-7c axis.

IL-6/STAT3 signalling pathway regulates many biological processes, such as cell apoptosis and proliferation. Abnormal activation of IL-6/STAT3 was closely related to tumour angiogenesis and tumour migration (Hu et al. 2019). As widely reported, the IL-6/STAT3 pathway participates in the regulation of many malignant tumours, including liver cancer, pancreatic cancer, and ovarian cancer (Kao et al. 2015; Liu et al. 2016; Wang et al. 2016), as well as lung cancer (Deng et al. 2018). Studies showed that IL-6, TNF- α were tumour-associated cytokines and were elevated in the tumour microenvironment (Skrinjar et al. 2015). CuB significantly inhibited the expression levels of IL-6 and TNF- α in sepsis-induced acute lung injury (Hua et al. 2017). Our results showed the level of TNF- α in lung cancer cells was remarkably reduced by CuB treatment. Yang et al. (2017) showed that miR-218 overexpression inhibited cell proliferation and invasion as well as tumour growth *in vivo* by regulating IL-6 expression. What's more, IL-6 had a binding site to miR-let-7c. CuB could suppress the expression of IL-6, and overexpression of IL-6 could impair the regulatory effect of CuB on lung cancer cells.

Our research provided evidence that CuB suppressed lung cancer cell proliferation and promoted apoptosis by inhibiting XIST/miR-let-7c/IL-6/STAT3 axis. Thus, our study provided an effective treatment for lung cancer and clarified the specific mechanism, which may be of great significance for the diagnosis and treatment of lung cancer in the future.

Disclosure statement

The authors report no declarations of interest.

Funding

This work was supported by Self-financing Project of 2016 Science and Technology Support Plan of Hebei Provincial Department of Science and Technology (162777297).

Data availability statement

The datasets used or analyzed during the current study are available from the corresponding author on reasonable request.

References

- Alberg AJ, Samet JM. 2003. Epidemiology of lung cancer. *Chest*. 123(1 Suppl):21S–49S.
- Bhatt K, Mi QS, Dong Z. 2011. microRNAs in kidneys: biogenesis, regulation, and pathophysiological roles. *Amer J Physiol Renal Physiol*. 300(3): F602–F610.
- Bray F, Ferlay J, Soerjomataram I, Siegel RL, Torre LA, Jemal A. 2018. Global cancer statistics 2018: GLOBOCAN estimates of incidence and mortality worldwide for 36 cancers in 185 countries. *CA Cancer J Clin*. 68(6):394–424.
- Chae YK, Chang S, Ko T, Anker J, Agte S, Iams W, Choi WM, Lee K, Cruz M. 2018. Epithelial-mesenchymal transition (EMT) signature is inversely associated with T-cell infiltration in non-small cell lung cancer (NSCLC). *Sci Rep*. 8(1):2918.
- Chan KT, Meng FY, Li Q, Ho CY, Lam TS, To Y, Lee WH, Li M, Chu KH, Toh M. 2010. Cucurbitacin B induces apoptosis and S phase cell cycle arrest in BEL-7402 human hepatocellular carcinoma cells and is effective via oral administration. *Cancer Lett*. 294(1):118–124.
- Chen JC, Chiu MH, Nie RL, Cordell GA, Qiu SX. 2005. Cucurbitacins and cucurbitane glycosides: structures and biological activities. *Nat Prod Rep*. 22(3):386–399.
- Dandawate P, Subramaniam D, Panovich P, Standing D, Krishnamachary B, Kaushik G, Thomas SM, Dhar A, Weir SJ, Jensen RA, et al. 2020. Cucurbitacin B and I inhibits colon cancer growth by targeting the Notch signaling pathway. *Sci Rep*. 10(1):1290.
- Deng Y-M, Zhang H, Liang J-M, Xian H-B, Chen Z-C, Tang Y-C, Yang S, Feng W-N. 2018. IL-37 mediates the anti-tumor activity in non-small cell lung cancer through IL-6/STAT3 pathway. *J Appl Biomed*. 16(1):15–21.
- Dong J, Teng F, Guo W, Yang J, Ding G, Fu Z. 2018. lncRNA SNHG8 promotes the tumorigenesis and metastasis by sponging miR-149-5p and predicts tumor recurrence in hepatocellular carcinoma. *Cell Physiol Biochem*. 51(5):2262–2274.
- El-Senduny FF, Badria FA, El-Waseef AM, Chauhan SC, Halaweish F. 2016. Approach for chemosensitization of cisplatin-resistant ovarian cancer by cucurbitacin B. *Tumour Biol*. 37(1):685–698.
- Fang J, Sun CC, Gong C. 2016. Long noncoding RNA XIST acts as an oncogene in non-small cell lung cancer by epigenetically repressing KLF2 expression. *Biochem Biophys Res Commun*. 478(2):811–817.
- Garg S, Kaul SC, Wadhwa R. 2018. Cucurbitacin B and cancer intervention: Chemistry, biology and mechanisms. *Int J Oncol*. 52(1):19–37.
- Guo J, Zhao W, Hao W, Ren G, Lu J, Chen X. 2014. Cucurbitacin B induces DNA damage, G2/M phase arrest, and apoptosis mediated by reactive oxygen species (ROS) in leukemia K562 cells. *Anticancer Agents Med Chem*. 14(8):1146–1153.
- Hu W, Ru Z, Zhou Y, Xiao W, Sun R, Zhang S, Gao Y, Li X, Zhang X, Yang H. 2019. Lung cancer-derived extracellular vesicles induced myotube atrophy and adipocyte lipolysis via the extracellular IL-6-mediated STAT3 pathway. *Biochim Biophys Acta Mol Cell Biol Lipids*. 1864(8):1091–1102.
- Hua S, Liu X, Lv S, Wang Z. 2017. Protective effects of cucurbitacin B on acute lung injury induced by sepsis in rats. *Med Sci Monit*. 23:1355–1362.
- Iyer MK, Niknafs YS, Malik R, Singhal U, Sahu A, Hosono Y, Barrette TR, Prensner JR, Evans JR, Zhao S, et al. 2015. The landscape of long noncoding RNAs in the human transcriptome. *Nat Genet*. 47(3):199–208.
- Kao J-T, Feng C-L, Yu C-J, Tsai S-M, Hsu P-N, Chen Y-L, Wu Y-Y. 2015. IL-6, through p-STAT3 rather than p-STAT1, activates hepatocarcinogenesis and affects survival of hepatocellular carcinoma patients: a cohort study. *BMC Gastroenterol*. 15(1):50.
- Lai G-M, Ozols RF, Young RC, Hamilton TC. 1989. Effect of glutathione on DNA repair in cisplatin-resistant human ovarian cancer cell lines. *J Natl Cancer Inst*. 81(7):535–539.
- Lin Y, Li J, Ye S, Chen J, Zhang Y, Wang L, Xi Y, Bu S, Qiu X. 2018. lncRNA GACAT3 acts as a competing endogenous RNA of HMGA1 and alleviates cucurbitacin B-induced apoptosis of gastric cancer cells. *Gene*. 678:164–171.
- Liu P, Xiang Y, Liu X, Zhang T, Yang R, Chen S, Xu L, Yu Q, Zhao H, Zhang L, et al. 2019. Cucurbitacin B induces the lysosomal degradation of eGFR and suppresses the CIP2A/PP2A/Akt signaling axis in gefitinib-resistant non-small cell lung cancer. *Molecules*. 24(3):647.
- Liu S, Sun J, Cai B, Xi X, Yang L, Zhang Z, Feng Y, Sun Y. 2016. NANOG regulates epithelial-mesenchymal transition and chemoresistance through activation of the STAT3 pathway in epithelial ovarian cancer. *Tumour Biol*. 37(7):9671–9680.
- Luo H, Sun Y, Wei G, Luo J, Yang X, Liu W, Guo M, Chen R. 2015. Functional characterization of long noncoding RNA Lnc_bc060912 in human lung carcinoma cells. *Biochemistry*. 54(18):2895–2902.
- Prensner JR, Chinnaiyan AM. 2011. The emergence of lncRNAs in cancer biology. *Cancer Discov*. 1(5):391–407.
- Schaefer MH, Serrano L. 2016. Cell type-specific properties and environment shape tissue specificity of cancer genes. *Sci Rep*. 6:20707.
- Seifart C, Plagens A, Dempfle A, Clostermann U, Vogelmeier C, von Wichert P, Seifart U. 2005. TNF-alpha, TNF-beta, IL-6, and IL-10 polymorphisms in patients with lung cancer. *Dis Markers*. 21(3):157–165.
- Shang GS, Liu L, Qin YW. 2017. IL-6 and TNF- α promote metastasis of lung cancer by inducing epithelial-mesenchymal transition. *Oncol Lett*. 13(6): 4657–4660.
- Sharma P, Mehta M, Dhanjal DS, Kaur S, Gupta G, Singh H, Thangavelu L, Rajeshkumar S, Tambuwala M, Bakshi HA, et al. 2019. Emerging trends in the novel drug delivery approaches for the treatment of lung cancer. *Chem Biol Interact*. 309:108720.
- Shi Y, Wang Y, Luan W, Wang P, Tao T, Zhang J, Qian J, Liu N, You Y. 2014. Long non-coding RNA H19 promotes glioma cell invasion by deriving miR-675. *PLOS One*. 9(1):e86295.
- Skrinjar I, Brailo V, Vidovic-Juras D, Vucicevic-Boras V, Milenovic A. 2015. Evaluation of pretreatment serum interleukin-6 and tumour necrosis factor alpha as a potential biomarker for recurrence in patients with oral squamous cell carcinoma. *Med Oral Patol Oral Cir Bucal*. 20(4): e402–e407.
- Sun N, Zhang G, Liu Y. 2018. Long non-coding RNA XIST sponges miR-34a to promotes colon cancer progression via Wnt/ β -catenin signaling pathway. *Gene*. 665:141–148.
- Tang H, Ma M, Dai J, Cui C, Si L, Sheng X, Chi Z, Xu L, Yu S, Xu T, et al. 2019. miR-let-7b and miR-let-7c suppress tumorigenesis of human mucosal melanoma and enhance the sensitivity to chemotherapy. *J Exp Clin Cancer Res*. 38(1):212.
- Tang Y, He R, An J, Deng P, Huang L, Yang W. 2017. lncRNA XIST interacts with miR-140 to modulate lung cancer growth by targeting iASPP. *Oncol Rep*. 38(2):941–948.
- Wang H, Shen Q, Zhang X, Yang C, Cui S, Sun Y, Wang L, Fan X, Xu S. 2017. The long non-coding RNA XIST controls non-small cell lung cancer proliferation and invasion by modulating miR-186-5p. *Cell Physiol Biochem*. 41(6):2221–2229.
- Wang L, Li J, Li Y, Pang L-B. 2020. Hsa-let-7c exerts an anti-tumor function by negatively regulating ANP32E in lung adenocarcinoma. *Tissue Cell*. 65: 101372.
- Wang X, Sun W, Shen W, Xia M, Chen C, Xiang D, Ning B, Cui X, Li H, Li X, et al. 2016. Long non-coding RNA DILC regulates liver cancer stem cells via IL-6/STAT3 axis. *J Hepatol*. 64(6):1283–1294.
- Wu G-Q, Chai K-Q, Zhu X-M, Jiang H, Wang X, Xue Q, Zheng A-H, Zhou H-Y, Chen Y, Chen X-C, et al. 2016. Anti-cancer effects of curcumin on lung cancer through the inhibition of EZH2 and NOTCH1. *Oncotarget*. 7(18):26535–26550.
- Xu J, Yang S, Zhou T, Si Y, Xiang Y, Ke W, Zhang T, Liu X, Zhang L, Xiang K, et al. 2020. Cucurbitacin B inhibits gastric cancer progression by suppressing STAT3 activity. *Arch Biochem Biophys*. 684:108314.
- Xu X, Zhou X, Chen Z, Gao C, Zhao L, Cui Y. 2020. Silencing of lncRNA XIST inhibits non-small cell lung cancer growth and promotes chemosensitivity to cisplatin. *Aging*. 12(6):4711–4726.
- Yang Y, Ding L, Hu Q, Xia J, Sun J, Wang X, Xiong H, Gurbani D, Li L, Liu Y, et al. 2017. MicroRNA-218 functions as a tumor suppressor in lung cancer by targeting IL-6/STAT3 and negatively correlates with poor prognosis. *Mol Cancer*. 16:141.
- Yu T, Xu Y-Y, Zhang Y-Y, Li K-Y, Shao Y, Liu G. 2018. Plumbagin suppresses the human large cell lung cancer cell lines by inhibiting IL-6/STAT3 signaling *in vitro*. *Int Immunopharmacol*. 55:290–296.
- Zhang Y, Li X, Hou Y, Fang N, You J, Zhou Q. 2017. The lncRNA XIST exhibits oncogenic properties via regulation of miR-449a and Bcl-2 in human non-small cell lung cancer. *Acta Pharmacol Sin*. 38(3):371–381.
- Zheng P, Yin Z, Wu Y, Xu Y, Luo Y, Zhang T-C. 2018. lncRNA HOTAIR promotes cell migration and invasion by regulating MKL1 via inhibition miR206 expression in HeLa cells. *Cell Commun Signal*. 16(1):5.
- Zheng R, Lin S, Guan L, Yuan H, Liu K, Liu C, Ye W, Liao Y, Jia J, Zhang R. 2018. Long non-coding RNA XIST inhibited breast cancer cell growth, migration, and invasion via miR-155/CDX1 axis. *Biochem Biophys Res Commun*. 498(4):1002–1008.
- Zhou J, Zhao T, Ma L, Liang M, Guo Y-J, Zhao L-M. 2017. Cucurbitacin B and SCH772984 exhibit synergistic anti-pancreatic cancer activities by suppressing EGFR, PI3K/Akt/mTOR, STAT3 and ERK signaling. *Oncotarget*. 8(61):103167–103181.
- Zhu H, Zheng T, Yu J, Zhou L, Wang L. 2018. lncRNA XIST accelerates cervical cancer progression via upregulating Fus through competitively binding with miR-200a. *Biomed Pharmacother*. 105:789–797.